Connectivity Graphs as Models of Local Interactions*

Abubakr Muhammad and Magnus Egerstedt
{abubakr,magnus}@ece.gatech.edu
Department of Electrical and Computer Engineering
Georgia Institute of Technology
Atlanta, 30332 GA, USA

Abstract

In this paper, we study graphs that arise from certain sensory and communication limitations on the local interactions in multi-agent systems. In particular, we show that the set of graphs that can represent formations corresponds to a proper subset of all graphs and we denote such graphs as connectivity graphs. These graphs have a special structure that allows them to be composed from a small number of atomic generators using a certain kind of graph amalgamation. This structure moreover allows us to give connectivity graphs a topological characterization in terms of their simplicial complexes. Finally, we outline some applications of this topological characterization to the construction of decentralized algorithms.

1 Introduction

The problem of coordinating multiple mobile robots is one in which a finite representation of the configuration space appears naturally, namely by using graph-theoretic models for describing the local interactions in the formation. In other words, graph-based models can serve as a bridge between the continuous and the discrete when trying to manage the design-complexity associated with formation control problems. Notable results along these lines have been presented in [1, 2, 3], where graphs are used for modelling what neighboring robots a given robot can communicate with. In [4], the idea is to represent the desired formation as a graph, and then produce formations from free agents such that the appropriate links are formed between them. In [5], such graph-models were successfully used for showing how the use of nearest neighbor average heading rules asymptotically produced subgraphs in which all the robots maintained the same heading.

The conclusion to be drawn from these research efforts is that a number of questions can be answered in a natural way by abstracting away the continuous dynamics of the individual agents. In particular, if the existence of an edge between two agents corresponds to certain geometric relations such as spatial closeness, then the graphs are really dynamic in the sense that the time-driven evolution of the configuration space may result in the production of a new graph. Hence, by introducing a graph-based representation of the formation, one has in fact arrived at a hybrid dynamic system. Furthermore, information can be allowed to flow along the edges of the graph, thus resulting in a change of the time-driven dynamics based on events at the graph-level, which further stresses the hybrid nature of this construction.

In algebraic topology literature, the connectivity graphs appear as *nerves* of certain covers for sets. The concept of giving a topological representation to the union of a collection of sets is not new. Eduard Čech introduced his Čech - homology theory in 1932, which deals with such representations [10]. This work however remained un-noticed in applied sciences till it re-appeared in [6, 7] in the 1990's. In [6], unions of disks were considered, the nerve of which are exactly connectivity graphs and [7] describes some *kinetic data structures* that capture the changes in topology of dynamic connectivity graphs. However, it should be noted that this work differs from those mentioned above in many ways. Although Čech homology fully describes the topological shape of the collection of sets (or its dual, the connectivity graph), it is difficult to compute. The framework of connectivity graphs described below is easy to implement. More importantly, this framework is tailored specifically for implementation on a distributed (and decentralized) system of agents.

In this paper we show that the graphs that can represent formations do in fact correspond to a proper subset of all graphs, denoted by the set of connectivity graphs (Section 2), and that it is possible to give a topological characterization of such graphs in terms of their geometrical structure (Section 3) and their simplicial complexes (Sections 4 and 5). In the end (Section 6) we outline some applications of the theory developed in this paper, followed by the conclusions (Section 7).

2 Formations and Connectivity Graphs

Graphs can model local interactions between agents, when individual agents are constrained by limited knowledge of other agents. In this section we present a graph theoretic formalism for describing formations in which the primary limitation of perception for each agent is the range of its sensor. Suppose we have N such agents with identical dynamics evolving on $\mathbb{R}^2$. Each of the agents carries a pre-assigned unique identification tag $n \in \{1, 2, \ldots, N\}$. Each agent is also equipped with a range limited sensor by which it can sense the position of other agents. All agents have identical sensor ranges δ. Let the position of each agent be $x_n \in \mathbb{R}^2$, and its dynamics be given by

$$\dot{x}_n = f(x_n, u_n),$$

where $u_n \in \mathbb{R}^m$ is the control for agent n and $f : \mathbb{R}^2 \times \mathbb{R}^m \to \mathbb{R}^2$ is a smooth vector field. The configuration space $\mathcal{C}^N(\mathbb{R}^2)$ of the agent formation is made up of all ordered N-tuples in $\mathbb{R}^2$, with the property that no two points coincide, i.e.

$$\mathcal{C}^N(\mathbb{R}^2) = (\mathbb{R}^2 \times \mathbb{R}^2 \times \ldots \mathbb{R}^2) - \Delta,$$

where $\Delta = \{(x_1, x_2, \ldots, x_N) : x_i = x_j \text{ for some } i \neq j\}$. The evolution of the formation can be represented as a trajectory $\mathcal{F} : \mathbb{R}_+ \to \mathcal{C}^N(\mathbb{R}^2)$, usually written as $\mathcal{F}(t) = (x_1(t), x_2(t), \ldots x_N(t))$ to signify time evolution. The spatial relationship between agents can be represented as a graph in which the vertices of the graph represent the agents, and the pair of vertices on each edge tells us that the corresponding agents are within sensor range δ of each other (See Figure 1) However several formations may give the same graph. We make these ideas precise as follows.
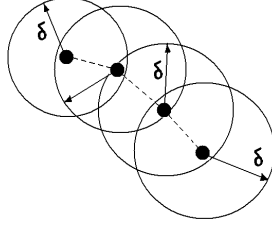

Figure 1: Agents and their connectivity graph.

Definition 2.1 (Connectivity Graph of a Formation) *Let $\mathcal{G}_N$ denote the space of all possible graphs that can be formed on N vertices $V = \{v_1, v_2, \ldots, v_N\}$. Then we can define a function $\Phi_N : C^N(\mathbb{R}^2) \to \mathcal{G}_N$, with $\Phi_N(\mathcal{F}(t)) = \mathcal{G}(t)$, where $\mathcal{G}(t) = (\mathcal{V}, \mathcal{E}(t)) \in \mathcal{G}_N$ is the connectivity graph of the formation $\mathcal{F}(t)$. $v_i \in \mathcal{V}$ represents agent i at position x_i, and $\mathcal{E}(t)$ denotes the edges of the graph. $e_{ij}(t) = e_{ji}(t) \in \mathcal{E}(t)$ if and only if $\|x_i(t) - x_j(t)\| \leq \delta$ $i \neq j$. In other words,*

$$\Phi_N(\mathcal{F}(t)) = (\{v_1, \ldots v_N\}, \{(v_i, v_j) \mid i \neq j \text{ and} \atop \|x_i(t) - x_j(t)\| \leq \delta\}) \tag{1}$$

Some observations about these connectivity graphs can be made already at this point.

- The graphs are *simple* by construction i.e. there are no loops or parallel edges.

- The graphs are always undirected because the sensor ranges are identical.

- The motion of agents in a formation may result in the removal or addition of edges in the graph. Therefore $\mathcal{G}(t)$ is a dynamic structure.

- Every graph in $\mathcal{G}_N$ is not a connectivity graph.

The last observation is not as obvious as the others, and it is analyzed in some detail below. While many researchers have referred to graphs of formations as their models; [1, 5]; the issue of whether an arbitrary graph corresponds to a proper agent formation has been mostly overlooked.

Definition 2.2 (Realization of a graph in $\mathcal{C}^N(\mathbb{R}^2)$) *A* realization *of a graph* $\mathcal{G} \in \mathcal{G}_N$ *is a formation* $\mathcal{F} \in \mathcal{C}^N(\mathbb{R}^2)$, *such that* $\Phi_N(\mathcal{F}) = \mathcal{G}$.

An arbitrary graph $\mathcal{G} \in \mathcal{G}_N$ can therefore be *realized* as a connectivity graph in $\mathcal{C}^N(\mathbb{R}^2)$ if $\Phi_N^{-1}(\mathcal{G})$ is nonempty. We denote by $\mathcal{G}_{N,\delta} \subseteq \mathcal{G}_N$, the space of all possible graphs on N agents with sensor range δ, that can be realized in $\mathcal{C}^N(\mathbb{R}^2)$. Let us start by analyzing this space for small values of N. For $N = 1$, the configuration space is $\mathcal{C}^1(\mathbb{R}^2) \simeq \mathbb{R}^2$ and the only possible graph on one agent is always realizable. For $N = 2$, the situation corresponds to whether the two agents are within δ distance of each other or not. Therefore all formations in the subset $\{(x_1, x_2) : \|x_1 - x_2\| \leq \delta, x_1 \neq x_2\} \subset \mathcal{C}^2(\mathbb{R}^2)$ correspond to the connected graph of 2 vertices, while the remaining configuration space corresponds to the situation when the graph is disconnected.
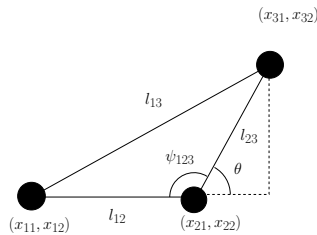

Figure 2: Depicted are three robots and their inter-robot distances.

If we now move on to the case for $N = 3$ similar constructions can be obtained for various connected and disconnected graphs on 3 vertices. Consider for example the situation in Figure 2, where the 3 agents are positioned at the points marked by circles. Let each position x_i be given by its Cartesian coordinate pair $(x_{i1}, x_{i2})^T$. For notational convenience let $\|x_1 - x_2\| = l_{12}$, $\|x_2 - x_3\| = l_{23}$ and $|x_1 - x_3\| = l_{13}$. Also let θ and ψ_{123} be the angles shown in the figure. In general, any connectivity graph on N vertices imposes various constraints on the relative positions of individual agents in the configuration space $\mathcal{C}^N(\mathbb{R}^2)$. In the case of a connected graph on 3 vertices, the constraints on positions x_1, x_2 and x_3 correspond to a single constraint on the angle ψ_{123}, when the the agents are positioned as shown in Figure 2. This simple observation will subsequently lead to some interesting properties of the connectivity graphs and their realizations. Suppose we are considering the line graph on 3 vertices

in Figure 4, then the given geometrical configuration corresponds to this graph if $l_{12} \leq \delta, l_{23} \leq \delta$, and $l_{13} > \delta$. Moreover we can write

$$
\begin{aligned}
l_{13}^2 &= (l_{12} + l_{23}\cos\theta)^2 + (l_{23}\sin\theta)^2, \\
&= l_{12}^2 + l_{23}^2 + 2l_{23}l_{12}\cos\theta.
\end{aligned}
$$

If $l_{13} > \delta$ then

$$
\cos\theta > \frac{\delta^2 - l_{12}^2 - l_{23}^2}{2l_{23}l_{12}}.
$$

It is easy to see that the term on the right has a minimum corresponding to the maximum values of $l_{12} = l_{23} = \delta$. Therefore $\cos\theta > -\frac{1}{2}$ which means that $\theta \in [-\frac{2\pi}{3}, \frac{2\pi}{3}]$. Therefore the smaller angle between l_{12} and l_{23} satisfies $\psi_{123} = \pi - \theta > \frac{\pi}{3}$, for all $0 < l_{12}, l_{23} \leq \delta$ and $l_{13} > \delta$. Hence, whenever we have two edges e_{ij} and e_{ik} in a connectivity graph that share a vertex v_i in such a way that there is no edge between vertices v_j and v_k, then

$$
\psi_{j,i,k} \triangleq \cos^{-1}\left(\frac{<x_j - x_i, x_i - x_k>}{\|x_j - x_i\|\|x_i - x_k\|}\right) > \frac{\pi}{3} \tag{2}
$$

Now, denote by S_N the "star graph" in $\mathcal{G}_N$ i.e. the graph which has $N-1$ vertices $v_2, v_3 \ldots v_N$ of degree 1 and one vertex v_1 with degree $N-1$. An example of such a graph is shown in Figure 3.a. Also denote by $\diamondsuit_5$ and $\diamondsuit_6$, the graphs in $\mathcal{G}_5$ and $\mathcal{G}_6$ respectively, as drawn in Figures 3.a and 3.b.
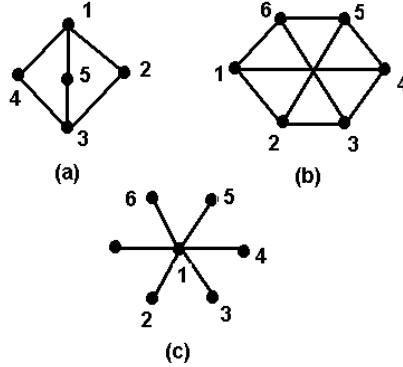

Figure 3: Graphs $\diamondsuit_5$, $\diamondsuit_6$ and S_7, that are not connectivity graphs

Proposition 2.1 *The graphs $\diamondsuit_5 \in \mathcal{G}_5$ and $\diamondsuit_6 \in \mathcal{G}_6$ do not belong to $\mathcal{G}_{5,\delta}$ and $\mathcal{G}_{6,\delta}$ respectively.*

Proof: Suppose that to the contrary $\diamondsuit_5 \in \mathcal{G}_{5,\delta}$ then there exists some realization $\mathcal{F} = (x_1, x_2, \cdots x_5) \in \mathcal{C}^5(\mathbb{R}^2)$ such that $\Phi_5(\mathcal{F}) = \diamondsuit_5$. From Equation

2 it follows that the angles ψ_{415}, ψ_{512}, ψ_{123}, ψ_{235}, ψ_{534} and ψ_{341} are all greater than $\frac{\pi}{3}$. Therefore,

$$\psi_{415} + \psi_{512} + \psi_{123} + \psi_{235} + \psi_{534} + \psi_{341} > 6\left(\frac{\pi}{3}\right) = 2\pi$$

But since $x_1, x_2, x_3, x_4 \in \mathbb{R}^2$ are vertices of a polygon of 4 sides, $\psi_{415} + \psi_{512} + \psi_{123} + \psi_{235} + \psi_{534} + \psi_{341} = 2\pi$ which is a contradiction. Therefore $\lozenge_5 \notin \mathcal{G}_{5,\delta}$.

Similarly if we assume that $\lozenge_6 \in \mathcal{G}_{6,\delta}$ then by a repeat of the above argument we get $\psi_{416} + \psi_{163} + \psi_{365} + \psi_{652} + \psi_{452} + \psi_{145} + \psi_{143} + \psi_{436} + \psi_{632} + \psi_{325} + \psi_{521} + \psi_{214} > 12\left(\frac{\pi}{3}\right) = 4\pi$. However from the condition that $x_1, x_2, \cdots, x_6 \in \mathbb{R}^2$ are vertices of a polygon of 6 sides, this sum should be exactly equal to 4π, which is a contradiction. Therefore $\lozenge_6 \notin \mathcal{G}_{6,\delta}$. ∎

Proposition 2.2 $\mathcal{S}_N \in \mathcal{G}_N$ *does not belong to* $\mathcal{G}_{N,\delta}$ *for* $N > 6$.

Proof: Suppose to the contrary, $\mathcal{S}_N \in \mathcal{G}_{N,\delta}$. If $deg(v_1) = N - 1$, and $(x_1, \cdots x_N) \in \mathcal{C}^N(\mathbb{R}^2)$ is a realization then $\psi_{i,1,j} > \frac{\pi}{3}$ for all $2 \leq i, j \leq N$. We have, $\psi_{2,1,3} + \psi_{3,1,4} + \cdots + \psi_{N-2,1,N-1} + \psi_{N-1,1,N} + \psi_{N,1,2} > (N-1)\pi/3$. If $N > 6$ then this sum is strictly greater than 2π. However by the given setup, this sum should be exactly equal to 2π. Therefore, by this contradiction $\mathcal{S}_N \notin \mathcal{G}_{N,\delta}$ for $N > 6$. ∎

There are of course many other examples of realizable and non-realizable connectivity graphs. If a graph is completely disconnected, it means that the distance between any two agents in the formation is separated by more than δ. This can easily be achieved by placing the vertices one by one in such a way that x_i does not belong to $\bigcup_{j=1}^{i-1} \mathcal{B}_\delta(x_j)$, where $\mathcal{B}_\delta(x)$ is the closed ball of radius δ centered at x. This observation can be further generalized as follows.

Lemma 2.1 *A graph* $\mathcal{G} \in \mathcal{G}_{N,\delta}$ *if and only if each of its connected component* $\mathcal{G}_i \in \mathcal{G}_{M_i}$ *is realizable in some* $\mathcal{G}_{M_i,\delta}$, $M_i < N$.

We omit a formal proof here for brevity but the concept is easy to understand. We saw earlier that completely disconnected graphs are trivially realizable by placing the agents further than δ from one another. If $\mathcal{G} \in \mathcal{G}_N$ has many disjoint connected components, say $\{\mathcal{G}_i\}$, we can place each connected component 'far away' from all other components so that none of the agents in one component can sense agents in other connected component. By this construction we have a realization for G if and only if all G_i have realizations in their respective spaces $G_{M_i,\delta}$.

Theorem 2.1 $\mathcal{G}_{N,\delta}$ *is a proper subspace of* $\mathcal{G}_N$ *if and only if* $N \geq 5$.

Proof: In order to prove that $\mathcal{G}_{N,\delta}$ is a proper subspace of $\mathcal{G}_N$ for some N, it is enough to show that $\Phi : C^N(\mathbb{R}^2) \to \mathcal{G}_N$ is not onto. Therefore we need to provide a graph $\mathcal{G} \in \mathcal{G}_N$ such that $\Phi^{-1}(\mathcal{G}) = \emptyset$. From Proposition 2.1, we have examples of graphs that are not realizable in $\mathcal{G}_{5,\delta}$ and $\mathcal{G}_{6,\delta}$. For $N \geq 7$ the

star graphs $\mathcal{S}_N$ of Proposition 2.2 provide the examples of graphs that cannot be realized as connectivity graphs in $\mathcal{G}_{N,\delta}$. This proves that $\mathcal{G}_{N,\delta}$ is a proper subspace of $\mathcal{G}_N$ if $N \geq 5$.

To prove that every graph in $\mathcal{G}_N$, for $N < 5$, is realizable in $\mathcal{G}_{N,\delta}$, we have to enumerate all possible graphs for $N < 5$ and give realizations for each graph. Since we are dealing with a small number $N(< 5)$, the enumeration strategy works well. The number of possible graphs to check can be further reduced by noting that we need to consider only connected graphs. The justification for this comes from Lemma 2.1 given above. In fact, from [8] we know what these graphs are, and they together with their realizations are given in Figures 4 and 5, which completes the proof. ∎
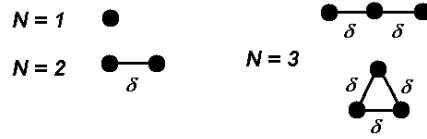

Figure 4: Possible realizations for all $G \in \mathcal{G}_{N,\delta}$ for $N \leq 3$
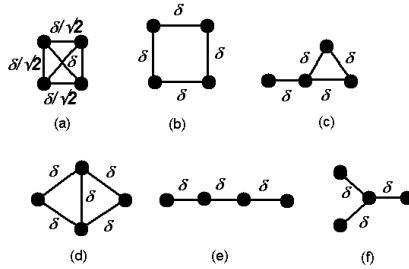

Figure 5: Possible realizations for all connectivity graphs in $\mathcal{G}_{4,\delta}$.

Corollary 2.1 *If each connected component $\mathcal{G}_i$ of a graph $\mathcal{G} \in \mathcal{G}_N$ belongs to $\mathcal{G}_{M_i}$, $M_i < 5$ then the graph has a realization in $\mathcal{G}_{N,\delta}$.*

Formations can produce a wide variety of graphs for N vertices. This includes graphs that have disconnected subgraphs or totally disconnected graphs with no edges. However the problem of switching between different formations or of finding interesting structures within a formation of sensor range limited agents can only be tackled if no sub-formation of agents is totally isolated from the rest of the formation [4]. This means that the connectivity graph $\mathcal{G}(t)$ of the formation $\mathcal{F}(t)$ should always remain *connected* (in the sense of connected graphs) for all time t. For notational convenience we use $\mathcal{G}_{N,\delta}^c \subseteq \mathcal{G}_{N,\delta} \subseteq \mathcal{G}_N$ to denote the set of all connected graphs of N vertices that satisfy the connectivity condition of the above definition for sensor range δ.

3 Geometric Structure of Connectivity Graphs

In this section we produce some results about the geometric structure of connectivity graphs. We will see that the graphs are made up of atomic graphs which, when combined in a certain way, produce more complex graphs. This decomposition will prove to be helpful in order to construct a *decentralized* method of obtaining a simplicial structure, buried inside the graph. This simplicial structure will consequently be used to associate a topological characterization to the connectivity graph.

Definition 3.1 (Image of a formation in $\mathbb{R}^2$) *If a given formation $\mathcal{F} = (x_1, x_2, \ldots x_N) \in \mathcal{C}^N(\mathbb{R}^2)$ has the connectivity graph $G = (\mathcal{V}, \mathcal{E}) = \Phi_N(\mathcal{F}(t))$, then each edge $e_k = \{v_{k_1}, v_{k_2}\} \in \mathcal{E}$ can be mapped to $\mathbb{R}^2$ by a map $f_k : \mathbb{R} \to \mathbb{R}^2$ given by $f_k(s) = sx_{k_1} + (1-s)x_{k_2}$ for $s \in [0,1]$. We call the image of the mapping f_k, the* image *of the edge in $\mathbb{R}^2$. The* image of a formation, $I_{\mathcal{F}} \subset \mathbb{R}^2$ *can be defined as the union of the images of all edges in the connectivity graph of the formation.*

$$I_{\mathcal{F}} = \bigcup_{e_k \in \mathcal{E}} f_k([0,1]) \subset \mathbb{R}^2. \tag{3}$$

Note that the image is constructed by mapping each vertex v_i of the graph to its position x_i and each edge $e_k = \{v_{k_1}, v_{k_2}\}$ to a line segment $sx_{k_1} + (1-s)x_{k_2}$, for $s \in [0,1]$, in $\mathbb{R}^2$. If it is clear from the context, what formation is under consideration, we will often write $I_{\mathcal{F}}$ as I_G, where $G = \Phi(\mathcal{F})$.

Sometimes it will be convenient to describe the image of a subgraph $H = (\mathcal{E}_H, \mathcal{V}_H)$ of the connectivity graph G of formation $\mathcal{F}$, where $\mathcal{E}_H \subset \mathcal{E}$ and $\mathcal{V}_H \subset \mathcal{V}$. In this case, we refer to the image of the subgraph H as

$$I_H = \bigcup_{e_k \in \mathcal{E}_H} f_k([0,1]) \subset \mathbb{R}^2, \ H \subseteq G = \Phi_N(\mathcal{F}) \in \mathcal{G}_{N,\delta}. \tag{4}$$

The image is thus what a graph would "look like" if drawn in the plane. Note that this is different from the concept of planar graphs [9] or imbedding graphs in $\mathbb{R}^2$ where edges are not necessarily mapped to straight lines. Two edges $e_i, e_j \in \mathcal{E}$ of a graph are said to be *crossing* if $f_i(s) = f_j(t)$ for some $s, t \in (0,1)$ and the set $f_i([0,1]) \cap f_j([0,1])$ has dimension 0. According to this definition, edge intersection at some vertex of the two edges does not count as a crossing. The condition that the intersection set is of dimension 0, rules out edge intersections of collinear points. For convenience denote by $e_i \bowtie e_j = \text{true}$, if $e_i, e_k \in \mathcal{E}$ are crossing edges. Given a formation $\mathcal{F}$ and its connectivity graph $\Phi(\mathcal{F}) = G = (\mathcal{E}, \mathcal{V})$, let $\mathcal{E}_\times \subseteq \mathcal{E}$ be the set of all crossing edges, and $\mathcal{V} \supseteq \mathcal{V}_\times = \{v \in \mathcal{V} \mid v \in e \text{ for some } e \in \mathcal{E}_\times\}$, then $H_\times = (\mathcal{E}_\times, \mathcal{V}_\times)$ is the subgraph of G made up of all crossing edges of the connectivity graph. We denote by $H_\triangle = (\mathcal{E} \setminus \mathcal{E}_\times, \mathcal{V})$, the subgraph of G consisting of all non-crossing edges so that $G = H_\times \cup H_\triangle$.

It should moreover be noted that the points in the image I_G can be categorized as smooth or non-smooth, where smoothness is defined in the setting
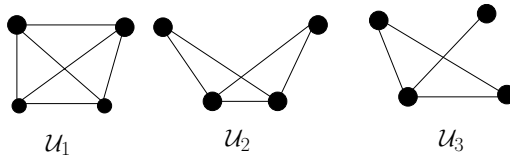
Figure 6: Crossing Generators.

of smooth manifolds. Any point x in the image that is not one of the robot positions $\{x_i\}_{i=1}^N$ or the crossing points is smooth, i.e. there always exists a small neighborhood $\mathcal{B}_\epsilon(x)$, and a homeomorphism $f : \mathcal{B}_\epsilon(x) \cap I_G \to \mathbb{R}$.

Proposition 3.1 *An image of a formation of 4 vertices has a pair of crossing edges only if its connectivity graph is isomorphic to either $\mathcal{U}_1, \mathcal{U}_2, \mathcal{U}_3$ as shown in Figure 6.*

Proof: From the Figures in 5, we see that only those connectivity graphs that are isomorphic to the graphs in Fig 6, namely those in 5.a 5.c and 5.d can be realized with crossing edges. For all other graphs in Figure 5, any attempt to create an image with crossing edges results in a violation of the constraints that define these graphs. ■

The three graphs $\mathcal{U}_1, \mathcal{U}_2, \mathcal{U}_3$ are called the *crossing generators* of all connectivity graphs. If G is a connectivity graph of a formation $\mathcal{F}$, and has two edges e_1, e_2 such that $e_1 \ltimes e_2 = \text{true}$, then there always exists a subgraph of G that contains e_1 and e_2 and is isomorphic to one of the crossing generators $\mathcal{U}_1, \mathcal{U}_2$ or $\mathcal{U}_3$. We now define the following operation.

Definition 3.2 (Δ-Amalgamation of crossing generators) *If $\mathcal{U}_i, \mathcal{U}_j \in \mathcal{G}_4$ are two crossing generators, $H \subset \mathcal{U}_i$ and $H' \subset \mathcal{U}_j$ are subgraphs s.t. $H, H' \simeq \mathcal{K}_3$ (the complete graph on 3 vertices), and there is an isomorphism $\Delta : H \to H'$ between the respective subgraphs, then their amalgamation (as standard amalgamation of two graphs [9]) according to the isomorphism Δ is called a Δ-amalgamation, denoted by $\mathcal{U}_i *_\Delta \mathcal{U}_j$.*

In the context of connectivity graphs of formations, Δ - amalgamation [1] is used as a description for unions of the type, $\bigcup_i I_{G_i}$, where each $G_i \subseteq G$, each G_i is a valid connectivity graph in $\mathcal{G}_{4,\delta}$ and each $G_i \simeq \mathcal{U}_j$ for some $1 \leq j \leq 3$. As explained in later sections, such amalgamations help characterize the geometrical constraints that give rise to crossing edges and non-smooth points in the image of a connectivity graph. They are used as an encoding method to describe the subgraph $H_\times = (\mathcal{E}_\times, \mathcal{V}_\times) \subseteq G$ made up of crossing edges. Therefore, we explain next, the kind of Δ-amalgamations appropriate to facilitate this encoding process, and hence the concept of a *well-defined Δ-amalgamation*.

---

[1]The letter Δ in the notation is used to emphasize that all amalgamations are done over triangular subgraphs.
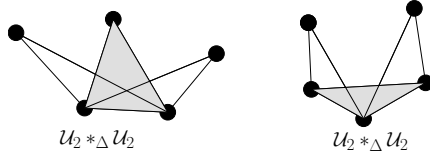
Figure 7: Different Δ-amalgamations of $\mathcal{U}_2$ and $\mathcal{U}_2$. The subgraphs involved in the Δ-amalgamations are shaded in gray.

It should be emphasized that there can be several ways to obtain Δ- amalgamations between any two crossing generators, depending on the choice of H and H'. Examples of such amalgamations are illustrated in the Figure 7, where the two crossing generators, both isomorphic to $\mathcal{U}_2$ produce two different Δ- amalgamations. The subgraphs involved in the Δ-amalgamations are shaded for ease of visualization. It should also be emphasized that every such Δ- amalgamation is not desirable. A sufficient condition for a Δ-amalgamation $G_{i_1} *_\Delta G_{i_2}$ to be *well- defined* is that $G_{i_1} *_\Delta G_{i_2}$ be a valid connectivity graph in $\mathcal{G}_{5,\delta}$. Generalizing this for an arbitrary number of amalgamations, if

$$\underbrace{G_{i_1} *_\Delta G_{i_2} *_\Delta \ldots G_{i_k}}_{(k-1)-amalgamations} \in \mathcal{G}_{4+k,\delta} \tag{5}$$

then the operation is well defined. Now consider the examples in the left-half of Figure 8. The three examples can be described by $\mathcal{U}_1 *_\Delta \mathcal{U}_1$, $\mathcal{U}_2 *_\Delta \mathcal{U}_2$ and $\mathcal{U}_3 *_\Delta \mathcal{U}_2 *_\Delta \mathcal{U}_3$ from top to bottom, and can nicely encode their respective subgraphs, that contain the crossing edges. The graphs in Figures 8.a and 8.c are not valid connectivity graphs. The constraints dictated by the respective graphs cannot result in valid formations in the configuration space. Similarly, the Δ-amalgamation drawn in Figure 8.e may or may not be valid. However, if we consider the graphs drawn on the right in Figures 8.b, 8.d and 8.f, the graphs are not only valid connectivity graphs but their crossing edges can also be encoded by the Δ-amalgamations described earlier. Based on this observation we define the following.

Definition 3.3 (Closure of a Δ-amalgamation) *Let $G_1 = (V_1, E_1)$, $G_2 = (V_2, E_2)$ denote two subgraphs of G. Let $\bar{V} = V_1 \cup V_2$, $\bar{E} = \{(v_i, v_j) \mid v_i, v_j \in \bar{V}\}$ and $\bar{G} = (\bar{V}, \bar{E})$. If $G_1 *_\Delta G_2$ is a Δ-amalgamation of G_1 and G_2, then the* Closure *of $G_1 *_\Delta G_2$ is defined as*

$$\overline{G_1 *_\Delta G_2} = (G_1 *_\Delta G_2) \cup \bar{G}.$$

In Figure 8, the graphs drawn on the right are closures of the graphs drawn on the left. If $\bar{G} = \emptyset$ then the Δ-amalgamation is equal to its closure. The graphs shown in Figure 7 and Figure 8.e can be such examples. We now give the following definition of a *well-defined* Δ-amalgamation.
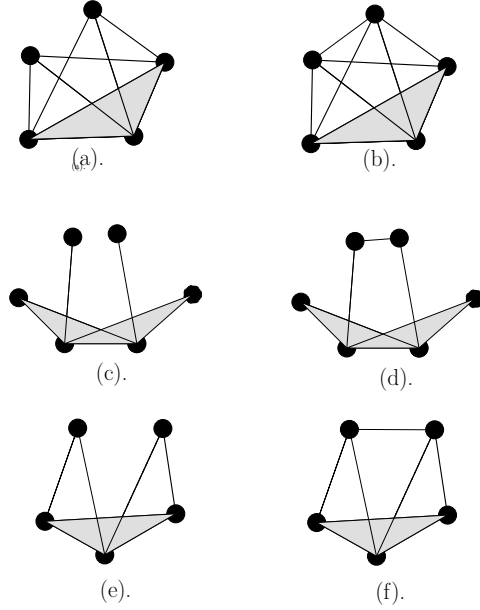
10

Figure 8: Examples of Δ-amalgamations (a,c,e) and their closures (b,d,f).

Definition 3.4 (Well-defined Δ-amalgamation) *A Δ-amalgamation of two subgraphs G_1, G_2 of a graph $G = H_\times \cup H_\Delta$, denoted by $G_1 *_\Delta G_2$ is well defined if*

$$\overline{G_1 *_\Delta G_2} = (G_1 *_\Delta G_2) \cup \bar{G} \in \mathcal{G}_{5,\delta},$$

and $\bar{E} \cap E_\times = \emptyset$.

In other words, a Δ-amalgamation is well-defined if it does not differ from its closure by any crossing edges. The Δ-amalgamation operation can be repeated to generate a whole family of graphs from the crossing generators, and is well-defined if the resulting graph's closure does not differ by any crossing edges. If we let $\Sigma = \sigma_1.\sigma_2.\ldots.\sigma_K$ be a finite string defined over $\{1, 2, 3\}$, then we denote a member of this family as:

$$\mathcal{G}_\Sigma = \mathcal{U}_{\sigma_1} *_\Delta \mathcal{U}_{\sigma_2} *_\Delta \ldots *_\Delta \mathcal{U}_{\sigma_K} \tag{6}$$

If we have repeated Δ-amalgamations of subgraphs of a connectivity graph, as in (5), there always exists a finite string Σ such that

$$\mathcal{G}_\Sigma \simeq G_{i_1} *_\Delta G_{i_2} *_\Delta \ldots G_{i_k} \subseteq \overline{G_{i_1} *_\Delta G_{i_2} *_\Delta \ldots G_{i_k}} \in \mathcal{G}_{4+k,\delta} \tag{7}$$

Each well-defined repeated Δ-amalgamation, as defined in (7), is called an *Atomic Crossing Graph*. Let $I_{\mathcal{G}_\Sigma}$ denote the image of a atomic crossing graph by referring to its isomorphic graph $\mathcal{G}_\Sigma$, when the details of the Δ-amalgamations is clear from context.

Proposition 3.2 *There exist a set of atomic crossing graphs $\{\mathcal{G}_{\Sigma_j}\}_{j \in J}$ such that*

$$I_{H_\times} \subset \bigcup_{j \in J} I_{\mathcal{G}_{\Sigma_j}} \subseteq I_G \subset \mathbb{R}^2, \tag{8}$$

where J is some finite indexing set, and each $x \in \left(I_{\mathcal{G}_{\Sigma_i}} \cap I_{\mathcal{G}_{\Sigma_j}} \right) \setminus \{x_k\}_{k=1}^N$ for $i, j \in J$, is smooth.

Proof: With slight abuse of notation, let $e \in G = (\mathcal{E}, \mathcal{V})$ denote that $e \in \mathcal{E}$. If $e_i \bowtie e_j =$ true, then denote by $H_q(e_i, e_j)$ the subgraph of G such that $H_q(e_i, e_j) \simeq \mathcal{U}_q$ for some $1 \leq q \leq 3$ and $e_i, e_j \in H_q(e_i, e_j)$. Also denote by $\mathcal{E}_{\Sigma_j}$ the set of edges for the graph $\mathcal{G}_{\Sigma_j}$. We now give the following algorithm to provide a constructive way of obtaining the atomic crossing graphs.

Algorithm 3.1 .

$A \; j \leftarrow 0$

$B \; \mathcal{E}_\times = \{e \in \mathcal{E} \mid e \bowtie e' =$ true for some $e' \in \mathcal{E}\}$

$C \;$ while $\mathcal{E}_\times \neq \emptyset$

    1. $j \leftarrow j + 1$

    2. $k \leftarrow 1$

    3. Pick $e_m \in \mathcal{E}_\times$

    4. Pick $e_p \in \mathcal{E}_\times$ such that $e_m \bowtie e_p =$ true

    5. $\mathcal{E}_\times \leftarrow \mathcal{E}_\times \setminus \{e_p, e_m\}$

    6. $\sigma_k = \arg\min_{1 \leq q \leq 3} (H_q(e_m, e_p))$

    7. $\Sigma_j \leftarrow \sigma_k$

    8. $\mathcal{G}_{\Sigma_j} \leftarrow H_{\sigma_k}(e_m, e_p)$

    9. $\mathcal{E}_{j_\circ} = \{e \in \mathcal{E}_\times \mid e \in H_{\sigma_k}(e_m, e_p)\}$

    10. $\mathcal{E}_\times \leftarrow \mathcal{E}_\times \setminus \mathcal{E}_{j_\circ}$

    11. $\mathcal{E}_{j_\times} = \{e \in \mathcal{E}_\times \mid e \bowtie e_l =$ true for some $e_l \in \mathcal{E}_{\Sigma_j}\}$

    12. while $\mathcal{E}_{j_\times} \neq \emptyset$

        (a) Pick $e_r \in \mathcal{E}_{j_\times}$

        (b) Pick $e_s \in \mathcal{E}_{\Sigma_j}$ such that $e_r \bowtie e_s =$ true

        (c) $\mathcal{E}_\times \leftarrow \mathcal{E}_\times \setminus \{e_r, e_s\}$

        (d) $\sigma_{k+1} = \arg\min_{1 \leq q \leq 3} (H_q(e_r, e_s))$

        (e) $\Sigma_j \leftarrow \Sigma_j \sigma_{k+1} = \sigma_1 \sigma_2 \ldots \sigma_k \sigma_{k+1}$

        (f) $\mathcal{G}_{\Sigma_j} \leftarrow \mathcal{G}_{\Sigma_j} *_\Delta H_{\sigma_{k+1}}(e_r, e_s)$

        (g) $\mathcal{E}_{j_\circ} = \{e \in \mathcal{E}_\times \mid e \in \mathcal{E}_{j_\times} \wedge e \in H_{\sigma_{k+1}}(e_r, e_s)\}$

        (h) $\mathcal{E}_\times \leftarrow \mathcal{E}_\times \setminus \mathcal{E}_{j_\circ}$

> (i) $\mathcal{E}_{j\times} = \{e \in \mathcal{E}_\times \mid e \bowtie e_l = true \text{ for some } e_l \in \mathcal{E}_{\Sigma_j}\}$
> (j) $k \leftarrow k + 1$
>
> 13. *end*
>
> *D end*

The algorithm can be explained as follows. First get the set $\mathcal{E}_\times$ of all crossing edges of the graph (Step B). Execute the algorithm until all crossing edges are taken care of, i.e. removed from $\mathcal{E}_\times$. Start by picking randomly a pair of crossing edges e_m and e_p in $\mathcal{E}_\times$. Next, obtain the maximal subgraph $H_{\sigma_k}(e_m, e_p)$ of G that contains the two edges, such that it is isomorphic to one of the crossing generators (Steps C.6 $\cdots$ C.8). This gives the starting point for generating an atomic crossing graph. Delete all edges in $\mathcal{E}_\times$ that are also contained in $H_{\sigma_k}(e_m, e_p)$. Next, find all edges in $\mathcal{E}_\times$ that cross with any edge in $H_{\sigma_k}(e_m, e_p)$ (Step C.11). Now, pick an edge from this set and one of its crossing edges, say e_r and e_s. The pair of crossing edges will again span a maximal subgraph $H_{\sigma_{k+1}}(e_r, e_s)$ isomorphic to one of the crossing generators (Step C.12.d). This new subgraph will always intersect the previously found subgraph $H_{\sigma_k}(e_m, e_p)$ over a subgraph isomorphic to $\mathcal{K}_3$. This lets us glue the two subgraphs together by a Δ-amalgamation operation (Step C.12.f). Again, remove the crossing edges that are part of the newly found edge set $\mathcal{E}_{j\circ}$ (Steps C.12.g, k). Next, find the crossing edges that cross any edge of the resulting Δ-amalgamation. Now, repeat once again the process of picking randomly a pair of crossing edges, finding their crossing generator and gluing it by repeated Δ-amalgamations. This process continues until no crossing edge remains that crosses any edge of the resulting repeated Δ-amalgamation. Delete all crossing edges that are used in this construction. In this way we get our first atomic crossing graph $\mathcal{G}_{\Sigma_1}$. Now, go back to the main loop and repeat the same process for any remaining crossing edges to get a whole family of atomic crossing graphs $\mathcal{G}_{\Sigma_1}, \mathcal{G}_{\Sigma_2} \cdots \mathcal{G}_{\Sigma_j}$, until $\mathcal{E}_\times = \emptyset$.

Since there are only finitely many crossing edges, this algorithm always terminates in less than $|\mathcal{E}_\times|/2$ number of Δ-amalgamations. By executing this algorithm, it is clear that all crossing edges are eventually absorbed into one of $\mathcal{G}_{\Sigma_i}$ in a finite number of steps so that $H_\times \subset \cup_{j \in J} \mathcal{G}_{\Sigma_j}$, and hence $I_{H_\times} \subset \bigcup_{j \in J} I_{\mathcal{G}_{\Sigma_j}} \subseteq I_G \subset \mathbb{R}^2$. ∎

The above discussion gives a decomposition of connectivity graphs in terms of crossing and non-crossing edges. An example of such decomposition is given in Figure 9. These properties will become useful for obtaining a simplicial representation of connectivity graphs, which will subsequently help in understanding the "topological shape" of formations as discussed in the following section.

4 Simplicial Complexes and Connectivity Graphs

It is a well known fact from algebraic topology [10] that the study of topological shapes of compact closed manifolds is synonymous to the study of triangulations
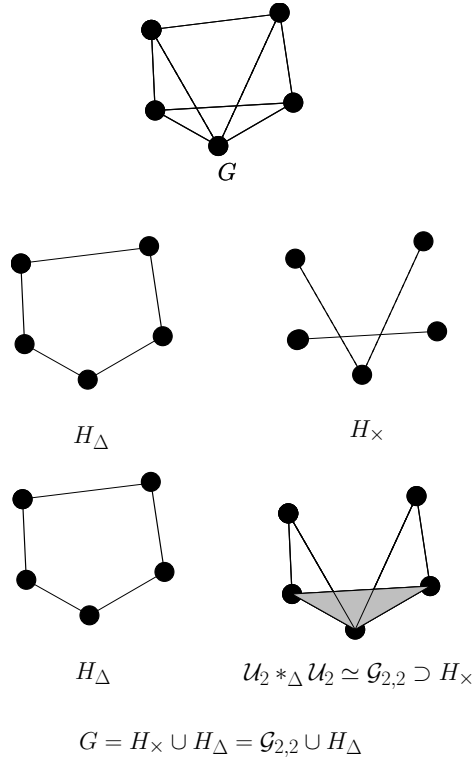
Figure 9: A connectivity graph and its decomposition in terms of atomic crossing graphs.

of manifolds. These triangulations are called simplicial complexes [11]. For the sake of clarity, we here give some background to such objects. A *k-simplex* is the smallest convex set that contains $k + 1$ points in general position [2] in $\mathbb{R}^k$. A finite collection of simplexes (of dimension less than or equal to n) in $\mathbb{R}^n$ is called a *simplicial complex* if whenever a simplex lies in the collection then so does each of its faces, and whenever two simplexes intersect, they do so in a common face. Associated with every simplicial complex K is a combinatorial object $\{\mathcal{V}, \mathcal{S}\}$ where $\mathcal{V}$ is the set of vertices of K and $\mathcal{S}$ the set of those subsets of $\mathcal{V}$ which span simplexes of K. The dimension of K is equal to the largest of the dimensions of its simplexes. Moreover, $\mathcal{S}$ has the following properties:

1. Each element of $\mathcal{V}$ belongs to $\mathcal{S}$. (A vertex is a 0-simplex.)

2. If S belong to $\mathcal{S}$ then so does any nonempty subset of S. (Any face of a simplex of K is itself in K.)

3. The sets in $\mathcal{S}$ are non-empty and have at most $dim(K) + 1$ elements.

---

[2]A set of points are in general position if any subset of them spans a strictly smaller hyperplane.

In line with the terminology developed in the preceding sections, K can be thought of as a *realization* of $\{\mathcal{V}, \mathcal{S}\}$. However, we will often write $K = \{\mathcal{V}, \mathcal{S}\}$ and overlook this subtle difference.

A simplicial complex of dimension 1 can be thought of as a graph whose image has no crossing edges. The only non-smooth points in the complex are the images of the vertices. Therefore, if some appropriate crossing edges are removed from a connectivity graph, its image is a well-defined simplicial complex. Proposition 3.2 leads to some conclusions along these lines. All points in the image I_{H_Δ} are smooth except the vertex points. This makes I_{H_Δ} a well defined simplicial complex of dimension 1. Therefore the problem of obtaining a simplicial representation for the graph is reduced to finding one for $I_{H_\times}$. If the image of each atomic crossing graph can be converted into a simplicial complex, by removal of images of crossing edges, then the union of the individual simplicial complexes would be a well-defined simplicial complex, as guaranteed by Proposition 3.2. Therefore the problem of obtaining a simplicial complex from a connectivity graph can be solved if each sub-problem of obtaining a simplicial complex for each atomic crossing graph can be solved.

Definition 4.1 (Simplicial Subgraph) *Every connectivity graph $G \in \mathcal{G}_{N,\delta}$ has at least one subgraph G_s which induces a well defined simplicial complex $K_{G_s} = (\mathcal{V}, \mathcal{S})$. We call G_s a simplicial subgraph of G.*

If a pair of vertices $S = \{v_i, v_j\}$ defines an edge in G_s then $S \in \mathcal{S}$. In other words every edge induces a 1-simplex in K_{G_s}. The subgraph of non-crossing edges $H_\Delta \subseteq G$, is also an example of a simplicial subgraph of G.

Definition 4.2 (Maximal Simplicial Subgraph) *A subgraph $G^* \subset G$ is said to be a maximal simplicial subgraph of G if there does not exist a simplicial subgraph of G that properly contains G^*.*

Before developing a method to obtain this maximal simplicial subgraph, a few points should be noted:

1. In order to preserve maximality, the removal of any non-crossing edge in the graph is not allowed.

2. Care has to be taken during the removal of crossing edges, as the removal of one crossing edge may result in the removal of all non-smooth points on another crossing edge, making the later non-crossing. Therefore the order in which crossing edges are removed is important.

3. The maximal simplicial subgraph of a connectivity graph is not unique and depends on the order in which crossing edges are removed.

We begin by considering the problem of obtaining maximal simplicial subgraphs of atomic crossing graphs.

Proposition 4.1 *There exists an algorithm to obtain a maximal simplicial subgraph of every atomic crossing graph.*

15

Proof: Let an atomic crossing graph $G = (\mathcal{E}, \mathcal{V})$ be isomorphic to G_Σ, as given by 7 or obtained by executing Algorithm 3.1, so that the string $\Sigma = \sigma_1 \sigma_2 \cdots \sigma_K$ gives the order of Δ-amalgamations in the atomic graph,

$$G_\Sigma \simeq G = G_1 *_\Delta G_2 *_\Delta \ldots G_K \in \mathcal{G}^c_{4+K,\delta},$$

where $G_k \simeq \mathcal{U}_{\sigma_k}$ for $1 \leq k \leq K$. Now execute the following algorithm.

Algorithm 4.1 .

1. $\mathcal{E}^* \leftarrow \mathcal{E}$

2. $G^* \leftarrow (\mathcal{E}^*, \mathcal{V})$

3. for $k = K$ to 1

    (a) $\mathcal{E}_\times = \{e \in G_k \mid e \bowtie e' = \text{true for some } e' \in G^* \setminus G_k\}$

    (b) $\mathcal{E}^* \leftarrow \mathcal{E}^* \setminus \mathcal{E}_\times$

    (c) $G^* \leftarrow (\mathcal{E}^*, \mathcal{V})$

    (d) $\mathcal{E}_\circ = \{e \in G^* \cap G_k \mid e \bowtie e' = \text{true for some } e' \in G^* \cap G_k\}$

    (e) if $|\mathcal{E}_\circ| = 2$ then

        i. $\{e_1, e_2\} \leftarrow \mathcal{E}_\circ$
        ii. $\mathcal{E}^* \leftarrow \mathcal{E}^* \setminus e_1$
        iii. $G^* \leftarrow (\mathcal{E}^*, \mathcal{V})$

    (f) end

4. end

The algorithm can be explained as follows. In each iteration k of the loop, first get the edges in the $G_k \simeq \mathcal{U}_{\sigma_k}$ that intersect any edge of the remaining graph $G^* \setminus G_k$ (Step 3.a). These are all crossing edges in G_k that need not intersect any other edge in G_k. Remove these edges from $\mathcal{E}^*$ and update G^* (Step 3.c). Now find any remaining crossing edges in $G^* \cap G_k$ (Step 3.d). Any edges found in this step would be a subset of the crossing edges, out of which the crossing generator was originally constructed by Algorithm 3.1 or by (7). In fact, only two possibilities can occur. Either both crossing edges are removed in Step 3.b if they both intersected with some other edges in $G^* \setminus G_k$, so that $|\mathcal{E}_\circ| = 0$. Or, both edges are obtained if they only cross each other so that $|\mathcal{E}_\circ| = 2$. The case $|\mathcal{E}_\circ| = 1$ never happens because it needs 2 edges to obtain a crossing. When $|\mathcal{E}_\circ| = 2$, removing either of the two edges is equivalent and we follow the convention of removing the first edge in the set (Step 3.e.ii). The graph G^* is again updated. After k iterations of examining the crossing generators in the backward direction, we obtain $G^* = (\mathcal{E}^*, \mathcal{V})$. We will later denote it by G^*_Σ when the isomorphism G_Σ is considered. By construction, the algorithm fulfills all conditions for maximality as enumerated above. Therefore

the graph $G^* = (\mathcal{E}^*, \mathcal{V})$ obtained at the end of the algorithm is indeed the maximal simplicial subgraph of G. ∎

We now give our main result.

Theorem 4.1 *A maximal simplicial subgraph G^* of a connectivity graph $G \in \mathcal{G}_{N,\delta}$ is given by the union,*

$$G^* = \left(\bigcup_i G^*_{\Sigma_i} \right) \cup H_\triangle.$$

Proof: By Proposition 3.2 any crossing edge of a connectivity graph is contained in some atomic crossing graph G_{Σ_i} generated by repeated $\triangle$-amalgamations. Also by the same result, the intersection of the images of any two atomic crossing graphs G_{Σ_i} and G_{Σ_j} is made up of only smooth points (except the vertices). This means that the intersection of the two graphs has only non-crossing edges in common and the removal of crossing edges in one atomic crossing graph does not effect the crossing edges in the other graph. If we now obtain the maximal simplicial subgraph $G^*_{\Sigma_i}$ of each atomic crossing graph G_{Σ_i}, it does not result in the removal of any non-crossing edge in $G_{\Sigma_i} \cap G_{\Sigma_j}$. Therefore, if we obtain the maximal simplicial subgraph of each atomic crossing graph by executing Algorithm 4.1, then their union $\cup_i G^*_{\Sigma_i}$ is also maximal. Finally, the subgraph $H_\triangle$ contains no crossing edges and is already a maximal simplicial subgraph, thereby making

$$G^* = \left(\bigcup_i G^*_{\Sigma_i} \right) \cup H_\triangle,$$

a maximal simplicial subgraph of G. ∎

While the maximality condition captures the maximal simplicial structure in the connectivity graph, we can further see that any 3 vertices that span a triangle in G_s, can span a 2-simplex in the image. Therefore we have the following.

Definition 4.3 (Maximal Simplicial Complex) *$M_{G_*} = (\mathcal{V}, \mathcal{S})$ is the maximal simplicial complex spanned by a connectivity graph if:*

- *$\mathcal{S}_1 \subseteq \mathcal{S}$, where $(\mathcal{V}, \mathcal{S}_1)$ is the 1-simplicial complex of the maximal simplicial subgraph $G_* \subset G$.*

- *If a set of any three vertices $L = \{v_i, v_j, v_k\}$ form a cycle in $(\mathcal{V}, \mathcal{S}_1)$ then $L \in \mathcal{S}$*

The set of vertices $S = \{v_i, v_j, v_k\}$, that form a cycle in G_* induces a 2-simplex in K. Therefore M_{G_*} is a 2-complex made up of:

1. 1-simplexes induced by the edges of the graph

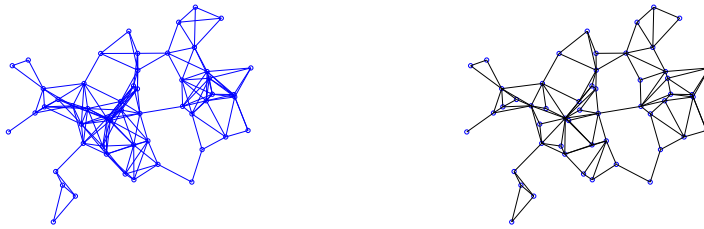2. 2-simplexes induced by the cycles of 3 vertices of the graph

17

Figure 10: A connectivity graph G. Figure 11: The maximal simplicial sub-graph G^*.

It may happen that M_{G_*} has no 2-simplexes. In this case the 1-skeleton is the complex itself case either. M_{G^*} is in fact the object associated with the topological shape of the formation. Some comments are appropriate at this point to explain why we have associated the topological characterization of the formation with the maximal simplicial complex spanned by its connectivity graph. Compare the lower connectivity graph on 3 vertices in Figure 4 with the graph in Figure 5.b. Both have a cyclic ring-like structure, which apparently makes them topologically equivalent. However, there is a subtle difference between the two, if we also desire that this structure is a decentralized multi-agent system. In the former example, all nodes interact directly with each other, whereas in the latter any node interacts directly with its two adjacent nodes only. Therefore the absence of an edge between opposite nodes creates a "hole" in the topological shape. By the method described in Definition 4.3, there would be a 2-simplex attached to the image of the graph of Figure 4 to get its maximal simplicial complex, making it a topological object of genus 0. On the other hand the maximal simplicial complex of the graph in Figure 5.b. would still have a hole (genus 1). Definition 4.3 lets us expand this point of view to more complex graphs. For example, the graph in Figure 10 has 3 holes, each of which is bounded by 4 nodes or more, as seen in its maximal simplicial complex in Figure 12. Once we have the simplicial complex of a graph, it can be studied using tools from standard algebraic topology to obtain its genus, fundamental groups, homological groups, etc. This point of view of topological characterization is also consistent with Čech homology based on set intersections [6]. The process of ignoring the crossing edges corresponds to ignoring simplexes of higher dimension in the connectivity graph, which simplifies the computations. Furthermore, the characterization of the topological shape in terms of "holes" gives an indication of the absence or presence of coverage in an area enclosed by a network of spatially distributed sensors. Therefore, the connectivity graph and its maximal simplicial complex are computationally cheap tools to answer the same question without computing set intersections, as required by Čech homology theory. However, before we give this type of topological characterization to connectivity graphs, we should investigate the issue of uniqueness for such characterization.
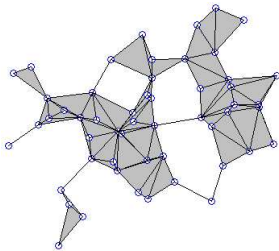
Figure 12: The maximal simplicial complex M_{G^*} spanned by the connectivity graph of Figure 10.

5   Uniqueness of Topological Characterization

It should be noted that maximal simplicial subgraph of a connectivity graph (and therefore the maximal simplicial complex) need not be unique and depends on the order in which crossing edges are removed, i.e. the order in which Δ-amalgamations are repeated to obtain each atomic crossing graph. For example, consider the situation in Figure 9. Starting with the connectivity graph G shown there, we can obtain a decomposition of the graph G using atomic crossing generators by executing Algorithm 3.1. It can be seen that A maximal simplicial subgraph can be obtained by executing Algorithm 4.1. The resulting graph G_1^* is depicted in Figure 13.a. However, upon close examination we can see that the subgraph G_2^* shown in Figure 13.b is also maximal. This should not come as a surprise, as different maximal simplicial graphs emerge as a result of the removal of crossing edges in different order. Now, consider the maximal simplicial complexes associated with the two maximal simplicial subgraphs, as shown in Figures 13.c and 13.d. It is obvious from the figures that the two simplicial complexes differ in their fundamental groups and hence in genus. The maximal simplicial complex of the subgraph obtained as a result of executing Algorithm 4.1 has genus 1, whereas the one depicted in Figure 13.d has a trivial fundamental group and hence genus 0. [3] Therefore, the choice exercised in removal of crossing edges makes a difference in the topological characterization of the connectivity graph. As explained above, the presence or absence of a "hole" in the simplicial complex is an indicator of presence or absence of direct interaction between nodes of a connectivity graph. Since we are interested in obtaining a topological characterization that truly captures the lack or presence of direct interactions, we must modify Algorithms 3.1 and 4.1. For obtaining such a modification, we define a quotient space on Δ-amalgamations as follows.

We first define the following equivalence relation. Let $G_1 *_\Delta G_2$ and $H_1 *_\Delta H_2$ be two well-defined Δ-amalgamations, then $G_1 *_\Delta G_2 \sim H_1 *_\Delta H_2$ if and only if:

1. $G_i \simeq H_i \simeq \mathcal{U}_{\sigma_i}$ for some $\sigma_i \in \{1, 2, 3\}$, and for $i = 1, 2$.

---

[3]For details on how to calculate fundamental groups of simplicial complexes, see [11, 10].
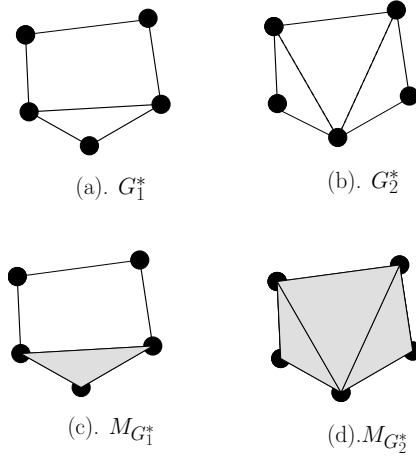
Figure 13: Two maximal simplicial complexes of the same connectivity graph

2. $G_1 *_\Delta G_2 \simeq H_1 *_\Delta H_2 \simeq \mathcal{U}_{\sigma_1} *_\Delta \mathcal{U}_{\sigma_2}$.

3. Number of non-smooth points in $I_{G_1 *_\Delta G_2}$ is equal to the number of non-smooth points in $I_{H_1 *_\Delta H_2}$.

The members of an equivalence class under this equivalence relation is denoted by $[G_1 *_\Delta G_2]$. We also define a quotient map π that sends $G_1 *_\Delta G_2$ to $[G_1 *_\Delta G_2]$. If we denote the space of all well-defined Δ-amalgamations between crossing generators as $\mathcal{U} *_\Delta \mathcal{U}$, then the resulting quotient space can be denoted by $\mathcal{U} *_\Delta \mathcal{U}/_\sim$. By enumeration techniques it can be seen that the quotient space is composed of only 7 equivalence classes, as shown in figure Figure 14. The details of this enumeration are omitted here for brevity.

Now let us define a map $\varphi : \mathcal{U} *_\Delta \mathcal{U}/_\sim \longrightarrow \mathcal{G}_5$ as depicted in Figure 15. This map is used to remove crossing edges whenever the crossing edges of a connectivity graph are captured as atomic crossing graphs. Since, π is also a graph isomorphism, it makes sense to consider the map $\pi^{-1}|_{\varphi(.)}$ which translates the edge removal back to the original graph. We have the following commutative diagram.

$$
\begin{array}{ccc}
\mathcal{U} *_\Delta \mathcal{U} & \xrightarrow{\varphi_*} & \mathcal{G}_5 \\
\downarrow{\pi} & & \uparrow{\pi^{-1}} \\
\mathcal{U} *_\Delta \mathcal{U}/_\sim & \xrightarrow{\varphi} & \mathcal{G}_5
\end{array}
$$

Thus, if $G_1, G_2 \subset G$, and $G_1 *_\Delta G_2$ is well-defined then, we can obtain a maximal simplicial subgraph of $\overline{G_1 *_\Delta G_2}$ using the map $\varphi_* = \pi^{-1} \circ \varphi \circ \pi$, i.e. $\varphi_*(G_1 *_\Delta G_2)$ is a maximal simplicial subgraph of $\overline{G_1 *_\Delta G_2}$. For repeated well-defined Δ-amalgamations, of the type given in (7), the Algorithm 4.1 can be modified as follows.

20
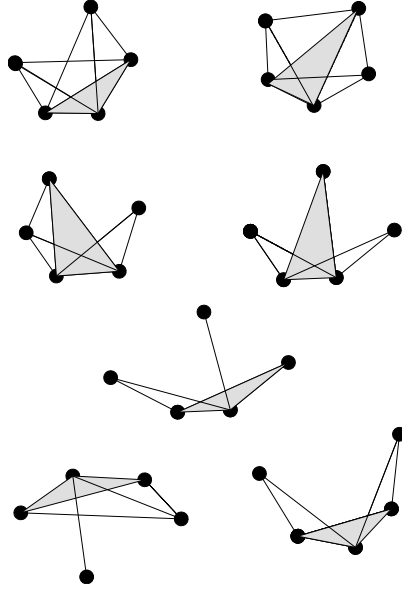
Figure 14: Members of the quotient space $\mathcal{U} *_\Delta \mathcal{U}/_\sim$

Algorithm 5.1 .

1. $G^* \leftarrow \emptyset$

2. *for* $k = K$ *to* 2

    (a) $G^* \leftarrow G^* \cup \varphi_*(G_{i_{k-1}} *_\Delta G_{i_k})$

3. *end*

Therefore the maximal simplicial subgraph of $\overline{G_{i_1} *_\Delta G_{i_2} *_\Delta \ldots G_{i_k}} \in \mathcal{G}_{4+k,\delta}$ can be obtained by

$$\bigcup_{j=1}^{k-1} \varphi_*(G_{i_j} *_\Delta G_{i_{j+1}})$$

The maximal simplicial subgraph obtained in this way is free of the inconsistencies explained earlier. One can now proceed to compute all sorts of topological invariants associated with the simplicial complex.

6 Applications of the Topological characterization of connectivity graphs

The geometric structure and topological characterization of the connectivity graphs of multi-agent formations given above, can be used to obtain certain
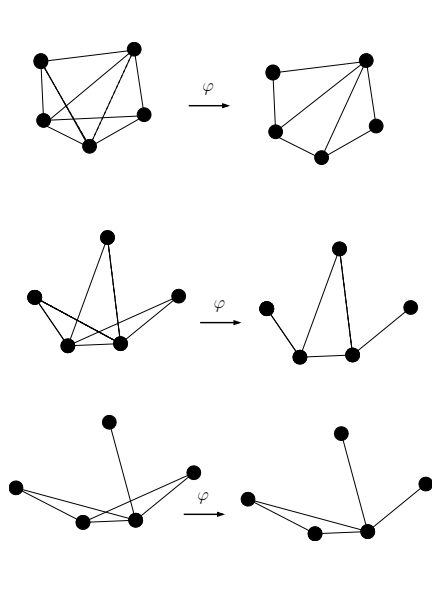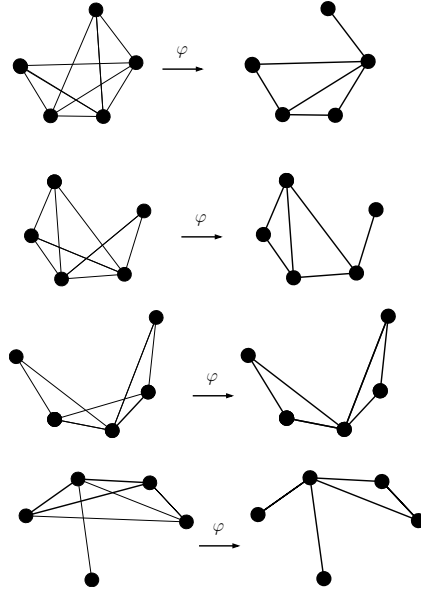
Figure 15:

Figure 16:

global properties of formations using decentralized algorithms, suitable for implementation on scalable, totally decentralized multi-agent systems. It will be appropriate to mention, that the entire machinery presented here for decomposing connectivity graphs into simplicial complexes becomes irrelevant, if the computations are performed in a centralized manner. The centralized method of obtaining the simplicial subgraph can be much simpler and need not have knowledge of the local geometrical structure obtained above. The maximal simplicial subgraph G^* of a connectivity graph $G \in \mathcal{G}_{N,\delta}$ can therefore be obtained using a decentralized algorithm. The detection of genus is also implementable as a decentralized algorithm. Since the fundamental group $\pi_1(I_{M_{G^*}})$ is isomorphic to the edge group $E(M_{G^*})$ of the triangulation, we can base our method on the reduction of loops inside M_{G^*}, according to the equivalence rules of $E(M_{G^*})$ [10]. Using this approach, one can implement a decentralized algorithm to find out if M_{G^*} has genus 0 or not. [12] The role of low-complexity formations called δ-chains (Hamiltonian paths) has moreover been studied and emphasized in a related work by the authors [13]. Decentralized algorithms for obtaining these δ-chains are of considerable interest to us and are a subject of current research. See Appendex for some preliminary results.

7 Conclusions

The connectivity graphs of formations, that arise due to sensory or communication limitations of individual agents have a rich set of structural and topological properties. These graphs are an important abstraction, as they let us capture various structural properties of the formations without referring to the actual positions of the agents. As the number of agents in a formation is increased beyond 4, numerous examples of graphs are obtained for which a realization is impossible that satisfy the given constraints. This tells us to be careful when using graph theoretic methods in even moderately large multi-agent systems. This work also gives us insight into the construction of various distributed algorithms which can be mapped on a decentralized multi-agent system.

Acknowledgments

References

[1] R. Saber and R. Murray, "Agreement Problems in Networks with Directed Graphs and Switching Topology," in *Proc. IEEE Conference on Decision and Control*, Maui, Hawaii, Dec. 2003.

[2] M. Mesbahi, "On a dynamic extension of the theory of graphs," in *Proc. American Control Conference*, Anchorage, Alaska, May, 2002.

[3] A Muhammad and M. Egerstedt, "Decentralized Coordination with Local Interactions: Some New Directions," in *Proc. Workshop on Cooperative Control*, Springer-Verlag, Block Island, RI, 2004. (To appear)

[4] E. Klavins, "Toward the Control of Self-Assemblinng Systems," *Control Problems in Agentics.* pp 153-168, Springer Verlag, 2002.

[5] A. Jadbabaie, J. Lin, and A. Morse, "Coordination of groups of mobile autonomous agents using nearest neighbor rules," *IEEE Transactions on Automatic Control*, Vol. 48, No. 6, pp. 988-1001, 2003.

[6] H. Edelsbrunner, "The Union of Balls and Its Dual Shape", *Discrete and Computational Geometry*, Vol 13, pp. 415-440, 1995.

[7] L. Guibas, J. Hershberger, S. Suri, and L. Zhang, "Kinetic Connectivity for Unit Disks", *Discrete and Computational Geometry*, Vol 25, pp. 591-610, 2001.

[8] L. Beinkeke and R. Wilson, *Graph Connections: Relationship between Graph theory and other areas of Mathematics*, Oxford, 1997.

[9] J. Gross J. and T. Tucker, *Topological Graph Theory*, John Wiley, 1987.

[10] A. Hatcher, *Algebraic Topology*, Cambridge University Press, 2002.

[11] M. Armstrong, *Basic Topology*, Springer-Verlag, 1983.

[12] A. Muhammad and M. Egerstedt, "On the Structure of Connectivity Graphs of Agent Formations," *Technical Report*, School of Electrical and Computer Engineering, Georgia Institute of Technology, Atlanta, GA, 2003.

[13] A. Muhammad and M. Egerstedt, "On the Structural Complexity of Multi-Agent Agent Formations," in *Proc. American Control Conference*, Boston, Massachusetts, USA, 2004.

A   Appendex

We have some preliminary results that suggest that the ability to obtain a simplicial representation of graphs lets us obtain δ-chains for an important class of connectivity graphs, namely the graphs whose maximal simplicial complex has genus 0. Some snapshots of the algorithm are given below convince the reader of the utility of the tools developed in this paper. As shown in the figures, the maximal simplicial subgraph is obtained during the initial steps of the algorithm, followed by the determination of genus (i.e. whether it has a genus 0 or not), and finally the construction of the δ-chain.
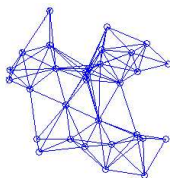

Figure 17: A connectivity graph.
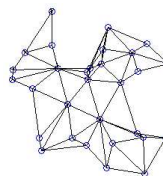

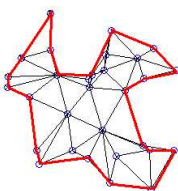Figure 18: Maximal simplicial subgraph of connectivity graph of 17.
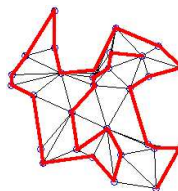

Figure 19: Boundary detection

Figure 20: Resulting δ-chain.

24